Absence of keratin 8 or 18 promotes antimitochondrial autoantibody formation in aging male mice

Diana M. Toivola,*[,1] Aida Habtezion,[†] Julia O. Misiorek,* Linxing Zhang,[†] Joel H. Nyström,* Orr Sharpe,[‡,§] William H. Robinson,[‡,§] Raymond Kwan,[¶,‖] and M. Bishr Omary[¶,‖]

*Department of Science and Engineering, Department of Biosciences, and Department of Cell Biology, Åbo Akademi University, Turku, Finland; [†]Division of Gastroenterology and Hepatology, [‡]Division of Immunology and Rheumatology, Stanford University School of Medicine, Palo Alto, California, USA; [§]Veterans Affairs Palo Alto Health Care System, Palo Alto, California, USA; [¶]Department of Molecular and Integrative Physiology, University of Michigan Medical School, Ann Arbor, Michigan, USA; and [‖]Veterans Affairs Ann Arbor Health Care System, Ann Arbor, Michigan, USA

ABSTRACT **Human mutations in keratin 8 (K8) and keratin 18 (K18), the intermediate filament proteins of hepatocytes, predispose to several liver diseases. K8-null mice develop chronic liver injury and fragile hepatocytes, dysfunctional mitochondria, and Th2-type colitis. We tested the hypothesis that autoantibody formation accompanies the liver damage that associates with K8/K18 absence. Sera from wild-type control, K8-null, and K18-null mice were analyzed by immunoblotting and immunofluorescence staining of cell and mouse tissue homogenates. Autoantibodies to several antigens were identified in 81% of K8-null male mice 8 mo or older. Similar autoantibodies were detected in aging K18-null male mice that had a related liver phenotype but normal colon compared with K8-null mice, suggesting that the autoantibodies are linked to liver rather than colonic disease. However, these autoantibodies were not observed in nontransgenic mice subjected to 4 chronic injury models. The autoantigens are ubiquitous and partition with mitochondria. Mass spectrometry and purified protein analysis identified, mitochondrial HMG-CoA synthase, aldehyde dehydrogenase, and catalase as the primary autoantigens, and glutamate dehydrogenase and epoxide hydrolase-2 as additional autoantigens. Therefore, absence of the hepatocyte keratins results in production of anti-mitochondrial autoantibodies (AMA) that recognize proteins involved in energy metabolism and oxidative stress, raising the possibility that AMA may be found in patients with keratin mutations that associate with liver and other diseases.—Toivola, D. M., Habtezion, A., Misiorek, J. O., Zhang, L., Nyström, J. H., Sharpe, O., Robinson, W. H., Kwan, R., Omary, M. B. Absence of keratin 8 or 18 promotes antimitochondrial autoantibody formation in aging male mice. *FASEB J.* 29, 5081–5089 (2015). www.fasebj.org**

Key Words: autoimmune liver disease · GDH · HMGCS2 · ALDH · intermediate filaments

Keratins make up the intermediate filament (IF) cytoskeleton of epithelial cells and include the obligate heteropolymeric keratin types I (keratins 9–28, 31–40) and II (keratins 1–8, keratins 71–80) (1). Simple-type epithelia, as found in the liver, pancreas, and intestine, express multiple keratins (keratins 7, 8, 18–20) (2, 3), but adult hepatocytes are unique because they express only keratin 8 (K8) and keratin 18 (K18) (3). The main function of keratins is to protect from cellular stress (4, 5) as supported by >80 human diseases that are caused or predisposed to by mutations in IF proteins (2, 6, 7). Human K8, K18 and K19 variants predispose to progression of several liver diseases including primary biliary cirrhosis (PBC) (8), hepatitis C virus infection (9), and acute liver failure (10). In contrast, the role of K8 mutations in inflammatory bowel disease (IBD) is less clear, likely due to functional redundancy of additional keratins (11). Multiple transgenic mouse models that lack keratins or express keratin mutants (3, 12) support the human disease relationship of K8/K18. For example, K8- or K18-null ($K8^{-/-}$, $K18^{-/-}$) mice develop spontaneous mild hepatitis (13–15) and are highly susceptible to apoptosis and toxin-mediated liver injury (16, 17). Both $K8^{-/-}$ and $K18^{-/-}$ mouse livers lack any K8 and K18 protein because the absence of one keratin causes proteosomal degradation of its partner keratin (18). Although the intestine appears normal in $K18^{-/-}$ mice (14), $K8^{-/-}$ mice develop a Th2-type ulcerative colitis, colorectal hyperproliferation, microflora-dependent decreased susceptibility to apoptosis, and mistargeting of subcellular proteins (13, 19–21). These intestinal manifestations are similarly observed in several IBD mouse models, including those lacking T-cell receptor-α (22) or IL-10 (23).

Abbreviations: ALDH, aldehyde dehydrogenase; AMA, antimitochondrial autoantibodies; GDH, glutamate dehydrogenase; HMGCS2, mitochondrial 3-hydroxy-3-methylglutaryl coenzyme A synthase; HRP, horseradish peroxidase; IBD, inflammatory bowel disease; IF, intermediate filament; K8, keratin 8; K18, keratin 18; $K8^{+/+}$, wild-type nontransgenic; $K8^{-/-}$, K8-null; $K18^{-/-}$, K18-null; MDB, Mallory-Denk bodies; NP-40, Nonidet P-40; PBC, primary biliary cirrhosis; PSC, primary sclerosing cholangitis

[1] Correspondence: Åbo Akademi University, Dept. Biosciences, Tykistökatu 6A, FIN-20520, Turku, Finland. E-mail: dtoivola@abo.fi

doi: 10.1096/fj.14-269795

This article includes supplemental data. Please visit *http://www.fasebj.org* to obtain this information.

Patients with IBD or liver autoimmune diseases often produce serum autoantibodies that are used in diagnosis (24, 25). Common autoantibodies in the autoimmune liver diseases primary sclerosing cholangitis (PSC), PBC, and autoimmune hepatitis include anti-mitochondrial autoantibodies (AMA), anti-nuclear antibodies, smooth muscle antibody, or antibody to liver kidney microsome type-1 (25, 26). Patients with IBD may also harbor serum antibodies including perinuclear anti-neutrophil cytoplasmic antibodies (in ulcerative colitis) and anti-*Saccharomyces cerevisiae* antibodies (in Crohn's disease) (24). The phenotypes of $K8^{-/-}$ mice that involve the colon and liver, coupled with the association of K8 variants with PBC (8), prompted us to hypothesize that autoantibody formation accompanies the liver damage associated with K8 or K18 absence in $K8^{-/-}$ and $K18^{-/-}$ mice. We validated this hypothesis by showing that aging male mice develop AMA, and we identified some of the autoantigen components recognized by these antibodies.

MATERIALS AND METHODS

Animal experiments and cells

$K8^{-/-}$, $K8^{+/-}$, wild-type $K8^{+/+}$ (13), and $K18^{-/-}$ mice were bred and genotyped as described elsewhere (13, 14). Mice that overexpress wild-type human K18 and mutant Arg90Cys human K18 (K18 R89C) (27) were also used. Mice received humane care, and their use was performed in accordance with the Committees on Use and Care of Animals. Tissue lysates generated from FVB/n mice were used for serum screening. Mice were also exposed to 4 different liver injury models, including: 1) a combined high-fat and high-carbohydrate diet that consists of a Surwit diet supplemented with fructose and sucrose (in the drinking water) for 14 wk as described elsewhere (28); 2) the established porphyrinogenic 3,5-diethoxycarbonyl-1,4-dihydrocollidine liver injury model in which mice were fed a powdered chow (Formulab Diet 5008, LabDiet, St. Louis, MO, USA) containing 0.1% diethoxycarbonyl dihydrocollidine (Sigma-Aldrich, St. Louis, MO, USA) for 3 mo (29); and the liver fibrosis models that involved administering 3) CCl_4 for 8 wk or 4) thioacetamide for 6 wk (30). Sera were collected and used for autoantibody screening as described below. Cell lines (American Type Culture Collection, Manassas, VA, USA) used included human Huh7 hepatoma and HT29 colon carcinoma cells, mouse NIH-3T3 fibroblasts and pancreatic LTDA cells. Cells were cultured at 37°C in media as recommended by the supplier.

Antibodies

Primary antibodies used were rabbit anti-superoxide dismutase 2 (SOD-2), anti-prohibitin (Abcam, Cambridge, MA, USA); anti-gpp130; anti-Hsp70 (Enzo Life Sciences, Farmingdale, NY, USA); rabbit anti-vinculin (Sigma-Aldrich); anti-catalase and anti-PMP70 (Thermo Fisher Scientific, Waltham, MA, USA); anti-cytochrome *c* (Cell Signaling, Danvers, MA, USA); anti-K8 and anti-K19 (Developmental Studies Hybridoma Bank, University of Iowa, Iowa City, IA, USA). Secondary antibodies were horseradish peroxidase (HRP)-conjugated anti-mouse IgG (Amersham Biosciences, Piscataway, NJ, USA); FITC-anti-mouse IgG and Texas Red-anti-rabbit (The Jackson Laboratory, Bar Harbor, ME, USA); and goat HRP-anti-mouse IgA, HRP-conjugated anti-IgA, anti-IgG or anti-IgM (Kirkegaard & Perry Laboratories, Gaithersburg, MD, USA).

Serum collection and screening for autoantibodies

Mice were euthanized by CO_2 inhalation, and blood was drawn by intracardiac puncture or from the submandibular vein using Golden rod lancets (MediPoint Inc., Mineola, NY, USA). Blood was collected in serum separator tubes (BD Microtainer; BD Biosciences, Franklin Lakes, NJ, USA), stored at 4°C overnight and centrifuged at 14,000 rpm (5 min) to obtain serum. Sera were portioned into aliquots and stored at −20°C. Individual sera were screened for immunoreactivity to mouse liver total lysates using SDS-PAGE and immunoblotting with the Miniblotter System (Immunetics, Boston, MA, USA). Sera were incubated at 1:200 dilution in 5% fat-free milk (2 h) in PBS (pH 7.4), then incubated with HRP-anti-mouse IgG and detected using the Enhanced Chemiluminescence Plus kit (Perkin Elmer, Waltham, MA, USA). Sera were scored as positive if a signal was obtained in the 40–60 kDa range matching control sera.

Tissue collection and histology

Mouse tissues were fixed in 10% formalin for histologic analysis, or snap-frozen in liquid nitrogen for protein analysis. Fixed tissues were processed for paraffin embedding, sectioned, and stained with hematoxylin and eosin. Livers were scored in a blinded fashion (A.H.) for pathologic changes including inflammation, necrosis, vacuoles, giant cells, fat, and hemorrhage using a 4-point scale (0–4, none to maximum changes per parameter).

Immunofluorescence staining

Subconfluent NIH-3T3 and HT29 cells were grown on glass cover slips. Cells were fixed with 4% paraformaldehyde (in PBS, pH 7.4) then rinsed with 0.2% Nonidet P-40 (NP-40) and blocked (2.5% bovine serum albumin in PBS). $K8^{-/-}$ and $K8^{+/+}$ mouse sera (1:30 dilutions) were used as primary antibodies, and nuclei were stained with Toto-3 (Invitrogen, Carlsbad, CA, USA). Liver tissue was fresh frozen in optimal cutting temperature compound, cryosectioned, fixed in −20°C acetone for 10 min, and stained as described above with anti-PMP70 antibodies and Draq5 (Cell Signaling, Danvers, MA, USA). Samples were analyzed by an LSM510 META confocal microscope (Carl Zeiss, Jena, Germany).

Protein solubility and trypsin digestion

Cells were lysed in 0.1% NP-40 buffer in PBS/5 mM EDTA, pH 7.5 (45 min, 4°C) and pelleted (14,000 rpm, 5 min), and the supernatant was collected (NP-40 soluble fraction) (31). The pellet was then solubilized in 0.1% Empigen/PBS, incubated, and pelleted as described previously to provide the Empigen-soluble and pellet (detergent-insoluble) fractions. The lysates were diluted in reducing Laemmli sample buffer and tested by blotting for reactivity to mouse sera. To test whether the autoantigen is a protein, the soluble fraction was incubated (37°C) with or without trypsin, followed by separation using 12% acrylamide gels. Antigen integrity was determined by blotting using the mouse sera.

Mitochondrial and peroxisome isolation and mass spectrometry

The liver mitochondrial fraction was isolated as described (32). Peroxisomes were isolated using a kit (Perox1, Sigma-Aldrich, as recommended by the supplier) from $K8^{+/+}$ and AMA-positive $K8^{-/-}$ mice (8-mo-old males) that were placed on a water-only diet for 18 h prior to isolation. Mitochondrial homogenates were

separated in 2 dimensions by isoelectric focusing (first dimension), then SDS-PAGE (second dimension). Identical gels were stained using Coomassie Brilliant Blue or transferred for immunoblotting using antibody-positive K8 sera. Antibody-reactive protein spots were excised from gels and/or the membrane, immersed with 100% acetonitrile, then digested overnight (37°C, 0.1 mg/ml trypsin) in 10 mM ammonium acetate containing 10% acetonitrile. The trypsinized proteins were identified using an Agilent 1100 LC mass spectrometry system (Agilent Technologies, Santa Clara, CA, USA). Mass spectrometry/mass spectrometry analysis was performed using the Spectrum Mill software (Agilent). A valid score ($P < 0.05$) is 13 for peptides and 20 for proteins, and a minimum of 2 valid peptides were counted for each protein.

Antigen identification approach

Immunofluorescence microscopy (as described above) was used to demonstrate that $K8^{-/-}$ or $K18^{-/-}$ autoantibody-positive mouse sera reacted with mitochondrial antigens. Serum autoantibody binding to the mitochondrial fraction was confirmed by immune blotting. Antigen confirmation was scored as positive if the purified test antigen bound selectively to autoantibody-positive mouse serum by immunoblotting of the test antibody with the purified antigen. Antigen verification was also carried out by testing whether preabsorption of the test AMA^{+} antibody with the purified protein decreased the reactivity of the autoantibody by immunoblotting. The purified antigens included glutamate dehydrogenase (GDH)1 (Sigma-Aldrich), mitochondrial 3-hydroxy-3-methylglutaryl coenzyme A synthase (HMGCS2; Genway, San Diego, CA, USA) and bovine catalase (Sigma-Aldrich). $K8^{-/-}$ serum was preabsorbed with the purified target proteins (7.5 μl serum + 1.38 μl protein at 1.45 μg/μl in 200 μl PBS-Tween). Samples were mixed for 30 min (22°C), then brought up to 1500 μl with PBS for immunoblotting of liver/cell lysates.

Statistics

The numbers are given as average ± SD, and statistical analysis was performed by Student's *t* test.

RESULTS

Autoantibodies are readily detected in sera of aging male $K8^{-/-}$ and $K18^{-/-}$ mice

To test whether $K8^{-/-}$ mice develop autoantibodies, sera from $K8^{-/-}$ and control $K8^{+/+}$ littermate mice were screened for autoantibodies by immunoblotting normal mouse liver lysates as potential antigen using 1:200 serum dilution. Among 10 pairs of mice, 60% of $K8^{-/-}$ mice but none of age- and sex-matched littermate $K8^{+/+}$ mice displayed consistent reactivity toward a major antigen in the 40–60 kDa range (**Fig. 1*A***). Screening of additional mice focusing on this molecular weight region confirmed the presence of a frequently occurring $K8^{-/-}$ autoantibody against a dominant autoantigen labeled as band C, and intermittent weaker reactivity toward 3 additional autoantigens labeled bands A, B, D (Fig. 1*B*). The autoantibodies were found in 57% of all random-selected and screened mice and in 81% of male mice 8 mo of age and older (Fig. 1*C*, *D*; **Table 1**), but rarely in young males or female $K8^{-/-}$ mice or in aging $K8^{+/+}$ mice (Fig. 1*D*, Table 1). No differences in antigen reactivity were noted if the liver lysates used were from male or female mice, young or old mice, wild-type or $K8^{-/-}$ mice (not shown). Using secondary antibodies against mouse IgA, IgG, and IgM, the autoantibodies were determined to be IgG (not shown).

We then used sera from $K18^{-/-}$ mice, which manifest only a liver phenotype (14, 15), to dissect whether the autoantibodies are related to the liver or colon phenotype in the $K8^{-/-}$ mice. Similar to $K8^{-/-}$ mice, 11- to 12-mo-old $K18^{-/-}$ male mice develop autoantibodies that correspond to antigen C at a frequency of 75% (Table 1, Fig. 1*D*). Histologic scoring showed a trend ($P = 0.18$) but no significant difference in liver damage in autoantibody-positive compared with autoantibody-negative male $K8^{-/-}$ and $K18^{-/-}$ mice (Supplemental Table 1). In addition, there was no difference in liver histology between male and female $K8^{-/-}$ mice (not shown). No autoantibodies were detected in sera of mice that overexpress human wild-type K18 or a K18 R90C mutation (not shown). Similarly, no consistent autoantibodies in the same molecular weight range were observed in sera of mice subjected to 4 independent chronic liver injury models (high fat, porphyrinogenic toxin and 2 fibrosis injury models; see Materials and Methods), and only few occasional mice manifested a weak signal (Supplemental Fig. 1). Even if mouse models may have lower titers than the human disease (33), the serum dilution of 1:200 we used gave a robust signal in positive mice. Taken together, $K8^{-/-}$ and $K18^{-/-}$ male mice produce upon aging serum IgG-type autoantibodies that recognize 40–60 kDa autoantigens.

The main autoantigen is a ubiquitous and soluble protein

To further characterize the autoantigens, representative C-antigen-reactive-sera from $K8^{-/-}$ mice and sera from $K8^{+/+}$ mice were used to detect antigens in various tissues and cell lines. Sera from $K8^{-/-}$ but not $K8^{+/+}$ mice recognized antigens in human and mouse cell lines of fibroblast, liver, colon, and exocrine pancreatic origin (Fig. 1*E*), where the only $K8^{-/-}$ mouse antigen signals detected (Fig. 1*E*) matched in molecular weight those of the mouse tissue in the 50 kDa range (not shown). A similar antigen was also detected in lysates of small intestine, colon, kidney, lung, heart, spleen, and brain (Supplemental Fig. 1).

To analyze the properties of the autoantigens, NIH-3T3 cell lysates were fractionated into detergent soluble (NP-40, Empigen) and insoluble fractions. The major C autoantigen is found primarily in the NP-40 fraction, in contrast to the IF protein vimentin, which is soluble primarily in the stronger detergent Empigen (Fig. 1*F*). The antigen recognized by $K8^{-/-}$ sera is a protein, because it is readily digested by trypsin in NIH-3T3 cell lysates after 5 min at 37°C (Fig. 1*G*). The $K8^{-/-}$ autoantigen is thus a ubiquitous protein that is readily solubilized by NP-40.

The $K8^{-/-}$ autoantigens are mitochondrial proteins

To determine the subcellular localization of the antigens recognized by the $K8^{-/-}$ autoantibodies, an immunofluorescence staining was performed on NIH-3T3 cells. Sera positive for the 40–60 kDa proteins manifested cytoplasmic reticular and perinuclear staining patterns (**Fig. 2*B, D***) not

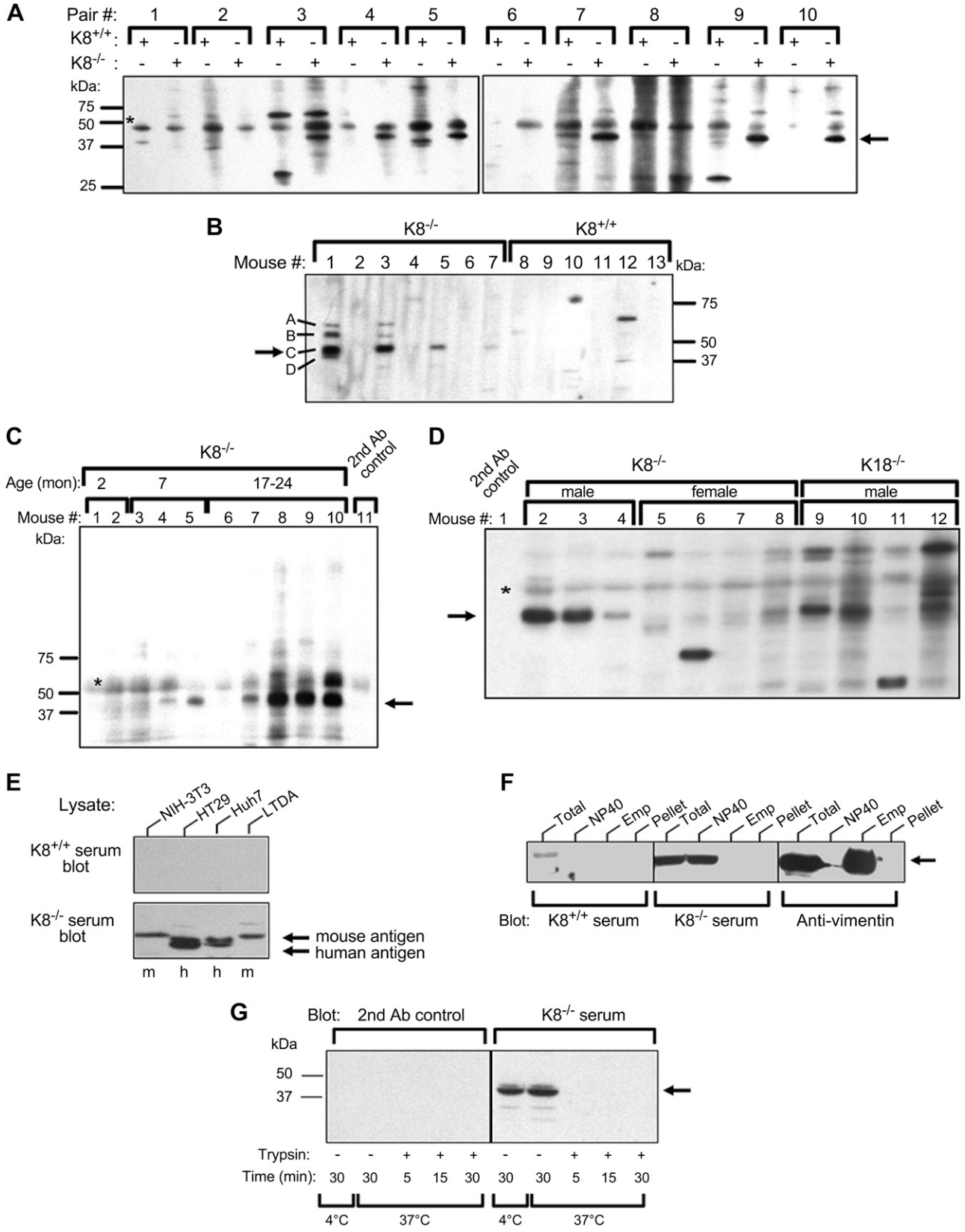

Figure 1. Autoantibodies are present in sera from aging K8$^{-/-}$ and K18$^{-/-}$ male mice. *A–D*) Sera from K8$^{+/+}$, K8$^{-/-}$, or K18$^{-/-}$ mice were analyzed by immunoblotting of total mouse liver lysates using a miniblotter setup. *A*) Ten age- and sex-matched K8$^{+/+}$ and K8$^{-/-}$ mouse pairs (Pair #) were analyzed, and the arrow points to a protein band (antigen) that is consistently observed only in K8$^{-/-}$ sera. *B*) Only male mouse serum is analyzed to test for autoantibodies, and bands marked A–D highlight the 4 major autoantigens recognized using K8$^{-/-}$ but not K8$^{+/+}$ sera. *C*) Sera from 10 male mice with the indicated ages were

(*continued on next page*)

TABLE 1. *Prevalence of autoantibodies recognizing 40-60 kDa liver antigens*

Genotype	Age (mo)	Total (*n*)	AMA positive		Phenotype	
			%	*n*	Liver	Colon
$K8^{+/+}$ M + F	2–18	51	6	3	N	N
$K8^{+/-}$ M + F	8–18	16	6	1	N	N/A[b]
$K8^{-/-}$ M + F[a]	2–7	16	0	0	A	A
M + F	8–24	60	57	34	A	A
M	8–24	27	81	22	A	A
F	8–24	6	0	0	A	A
$K18^{-/-}$ M	11–12	20	75	15	A	N

A, abnormal histology; N, normal histology. [a]Seventy-five percent males. [b]$K8^{+/-}$ colon appears normal but has a mild phenotype (19).

seen in antibody-negative $K8^{-/-}$ sera (Fig. 2*F*) or $K8^{+/+}$ sera (Fig. 2*A*, *C*, *E*). Similar results were obtained using HT29 cells (not shown). Costaining using autoantibody-positive $K8^{-/-}$ sera with markers for Golgi and mitochondria revealed primarily a mitochondrial distribution for the autoantigen (**Fig. 3*A***). Sera from a few $K8^{-/-}$ and $K18^{-/-}$ mice colocalized with ends of F-actin stress fibers and vinculin at filopodia (not shown). Occasional sera from aging mice carried autoantibodies to unidentified proteins (see Fig. 1), which were not further analyzed.

To biochemically identify the autoantigens, mouse liver mitochondria were purified by subcellular fractionation (Fig. 3*B*) and separated using 2-dimensional electrophoresis. The mitochondrial-enriched proteins were visualized by Coomassie Brilliant Blue staining (**Fig. 4*A***) and analyzed by immunoblotting using $K8^{-/-}$ sera (Fig. 4*B*) on parallel gels. The Coomassie Brilliant Blue-stained dots that colocalized with the immune-reactive spots were identified using mass spectrometry as GDH1 for antigen B and a mixture of mitochondrial HMG-CoA synthase (HMGCS2), catalase, and aldehyde dehydrogenase (ALDH) E2 for antigen C; the less abundant antigen A was identified as epoxide hydrolase 2 (**Table 2**).

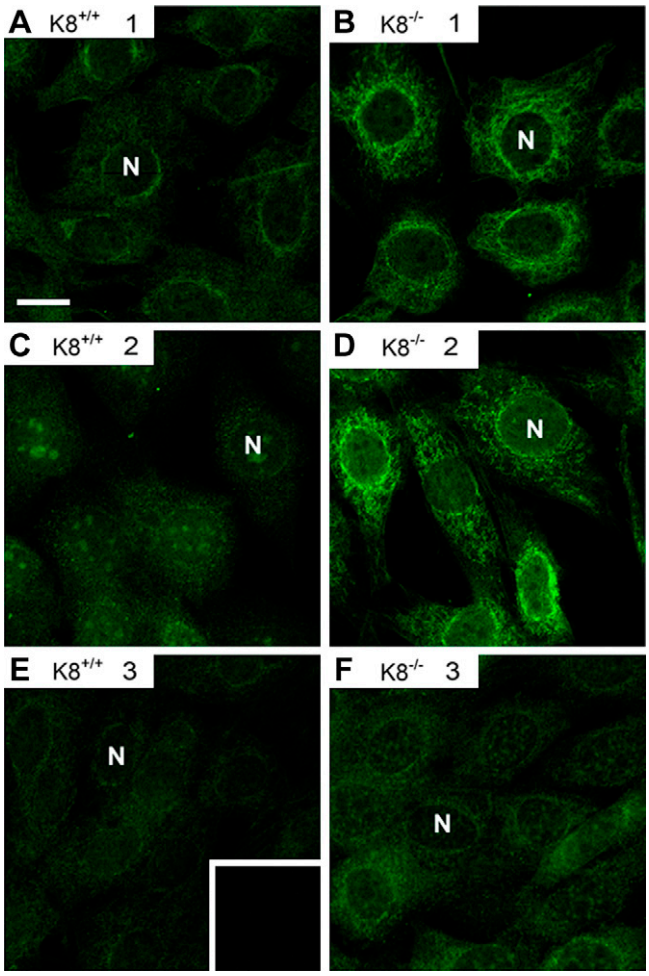

Figure 2. $K8^{-/-}$ mouse autoantibodies manifest a cytoplasmic reticular staining pattern. $K8^{+/+}$ (*A*, *C*, *E*) and $K8^{-/-}$ (*B*, *D*, *F*) sera from 3 mice (1–3) per genotype were used as primary antibodies to stain NIH-3T3 cells followed by FITC-labeled secondary anti-mouse antibody. The $K8^{-/-}$ sera were positive (*B*, *D*) or negative (*F*) for autoantibody reactivity as determined by immunoblotting. *E*) Insert represents secondary antibody alone control staining. N, nuclei.

Validation of GDH1 and HMGCS2 as primary autoantigens

To validate the identified antigens, the commercially purified GDH1 and HMGCS2 proteins were analyzed by 2 approaches: 1) directly by immunoblotting purified putative antigens with $K8^{-/-}$ mouse sera to determine if the autoantibody identifies these proteins as antigens, and 2) preabsorption of sera with purified GDH1 and HMGCS2 autoantigens. Autoantibodies against antigen B but not antigen C detected purified GDH1 (Fig. 4*C*). Preabsorption of antigen B sera using purified GDH1 diminished but did not completely remove the Western blot signal for GHD1, supporting that the B antigen corresponds in part to GDH1 (Fig. 4*D*). Likewise, bacterially expressed HMGCS2 loaded onto gels and probed with mouse serum shows that the $K8^{-/-}$ C sera reacts stronger with HMGCS2, compared with $K8^{+/+}$ serum (Fig. 4*E*). Preabsorption of 2 different $K8^{-/-}$ sera with HMGCS2 and probing of filters with $K8^{-/-}$ serum shows a decreased signal when the serum was preabsorbed (Fig. 4*F*). For catalase, also a minor decrease in C antigen signal in liver lysates was noted after incubation of the mouse serum with purified bovine catalase (not shown).

screened. *D*) Sera from aging (8 mo or older) $K8^{-/-}$ females and $K18^{-/-}$ male mice were tested for autoantibody presence using $K8^{-/-}$ as positive controls. The secondary (2nd) antibody control (lane 1) is indicated. *C*, *D*) Arrows highlight autoantigen C and asterisks (*), nonspecific signal. *E*) Mouse and human cell line lysates were tested by immunoblotting using sera from $K8^{-/-}$ and $K8^{+/+}$ mice. *F*) NIH-3T3 fibroblasts were sequentially solubilized with NP-40 then Empigen and further analyzed (together with the total cell fraction or the post-Empigen pellet) by immunoblotting with $K8^{+/+}$ or $K8^{-/-}$ serum, or anti-vimentin antibody as a control. *G*) NIH-3T3 NP-40 lysates were incubated with or without trypsin for the indicated times and then analyzed by immunoblotting using $K8^{-/-}$ serum or the secondary antibody control alone as a specificity control. Arrow highlights the autoantigen. Ab, antibody; Emp, Empigen; h, human; m, mouse; mon, month.

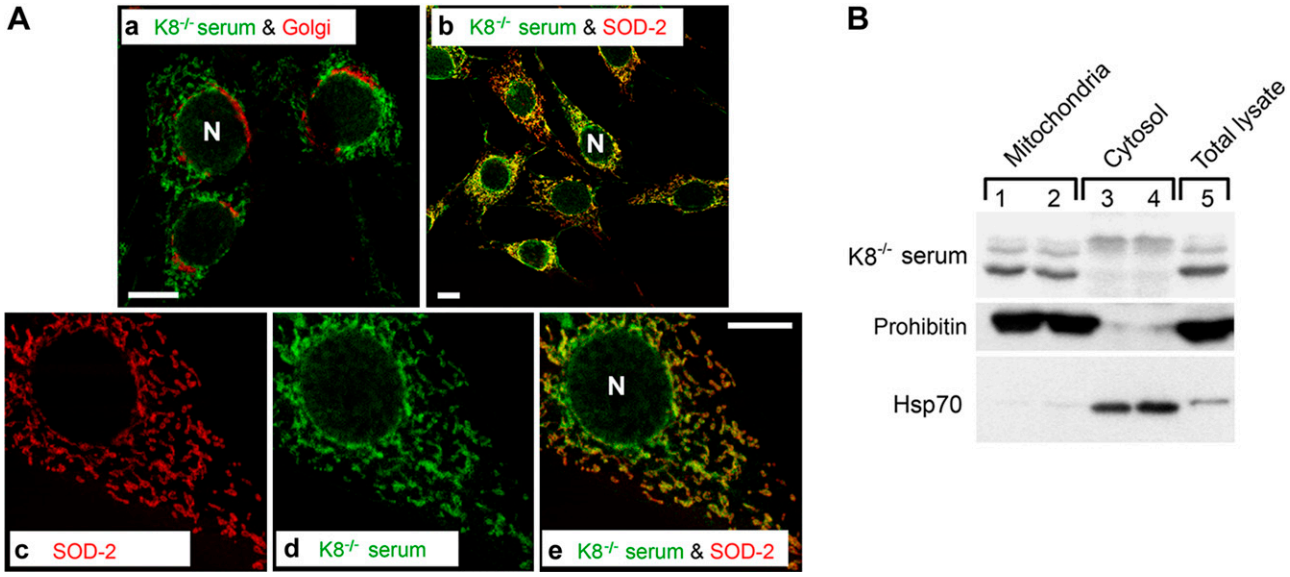

Figure 3. $K8^{-/-}$ sera recognize mitochondrial autoantigens. *A*) NIH-3T3 cells were double-stained with $K8^{-/-}$ serum (a, b, d, e; green) that tested positive for autoantigen-binding by immunoblotting, and the Golgi protein gpp130 (a; red) or the mitochondrial protein SOD-2 (b, c, e; red). The merged images of c and d illustrate colocalization of the autoantibody and SOD-2 (e; yellow). *B*) Mouse liver mitochondrial (lanes 1 and 2), cytosol (lanes 3 and 4), and total liver lysate (lane 5) fractions were blotted with serum from an antibody-positive $K8^{-/-}$ mouse, with prohibitin (mitochondrial marker) or Hsp70 (cytosolic marker). N, nuclei.

DISCUSSION

IF mutations cause or predispose to multiple tissue-specific human diseases, and these diseases parallel the tissue-specific expression of IFs and are phenocopied in IF-related genetic mouse models (3, 34). Some of the diseases have an autoimmune component; however, it is unknown whether the mouse models mimic the human disease in terms of presence of autoantibodies as has been described in other mouse models of autoimmune disease (26, 35). Our findings show that aging $K8^{-/-}$ and $K18^{-/-}$ male mice produce AMA at reasonably high titers. The liver is the likely source of autoantigens because $K8^{-/-}$ and $K18^{-/-}$ knockout mice both have a similar major phenotype in the liver (15), although $K8^{-/-}$ but not $K18^{-/-}$ mice also develop spontaneous colitis (13, 19–21). The liver phenotype, which has been extensively studied in $K8^{-/-}$ mice, includes predisposition to hepatotoxic injury (36–38) and apoptosis (16, 17) and profound hepatocyte fragility upon liver perfusion (39). Both genotypes have patchy loss of hepatocytes with replacement by multinucleated giant cells (15). $K18^{-/-}$ but not $K8^{-/-}$ mice develop spontaneous Mallory-Denk bodies (MDBs) with old age (14), thereby suggesting that the MDBs are not related to the AMA, albeit male mice are more susceptible to MDB formation (40). In the $K8^{-/-}$ and $K18^{-/-}$ livers, hepatocyte rather than biliary damage is likely the source of antigen exposure. The reason for this assessment is that there is no major pathology in the biliary system (not shown) (13) and bile ducts express primarily K19 and K7, in contrast to adult hepatocytes, which express only K8 and K18 (41), with the latter being more susceptible to injury in the absence of K8.

$K8^{-/-}$ hepatocyte mitochondria are smaller and irregularly distributed and have decreased ATP and cytochrome *c* levels (42), with altered hepatic glucose/glycogen metabolism (43). Notably, proteomic analysis of $K8^{-/-}$ hepatocytes (42) showed that 13 mitochondrial proteins had altered charged isoforms, including 3 of the autoantigens (GDH, ALDH, HMGCS2) we identified herein. It is likely that the keratin-dependent chronic mitochondrial stress and hepatocyte fragility lead to exposure of inner mitochondrial proteins to the immune system with consequent production of AMA, which highlights hepatocyte mitochondria as likely to be central in this phenotype. In PBC, where PBC-specific AMA is an important hallmark of disease and PDC-E2 the major antigen, the affected cholangiocyte apoptotic bodies are believed to be the antigen-presenting entity (26). The male preponderance of AMA in $K8^{-/-}/K18^{-/-}$ mice is unlike PBC, which is more frequent in females (44), but resembles PSC, which has a 2:1 male:female ratio and is typically associated with antineutrophil cytoplasmic antibodies rather than AMA (45). It is likely that sex-dependent human autoimmune diseases are related to hormonal causes, fetal microchimerism, or X-chromosome changes (26). Given that catalase is one of the autoantigens we observed, peroxisomal damage is also a potential source of the autoantigens. Notably, we did not observe an obvious alteration in the organization of peroxisomes or loss of the peroxisomal membrane protein PMP70 (based on immunofluorescence staining and immunoblotting, respectively; not shown). However, our findings cannot completely exclude the possibility of a peroxisomal defect that could contribute to the generation of the autoantibodies we observed.

The $K8^{-/-}/K18^{-/-}$ and the K18 R90C mice have either absent or disrupted cytoskeletal keratin networks, respectively. However, AMA were not found in K18 R90C mice, which raises the possibility that the presence of some keratins, albeit disorganized, is protective. However,

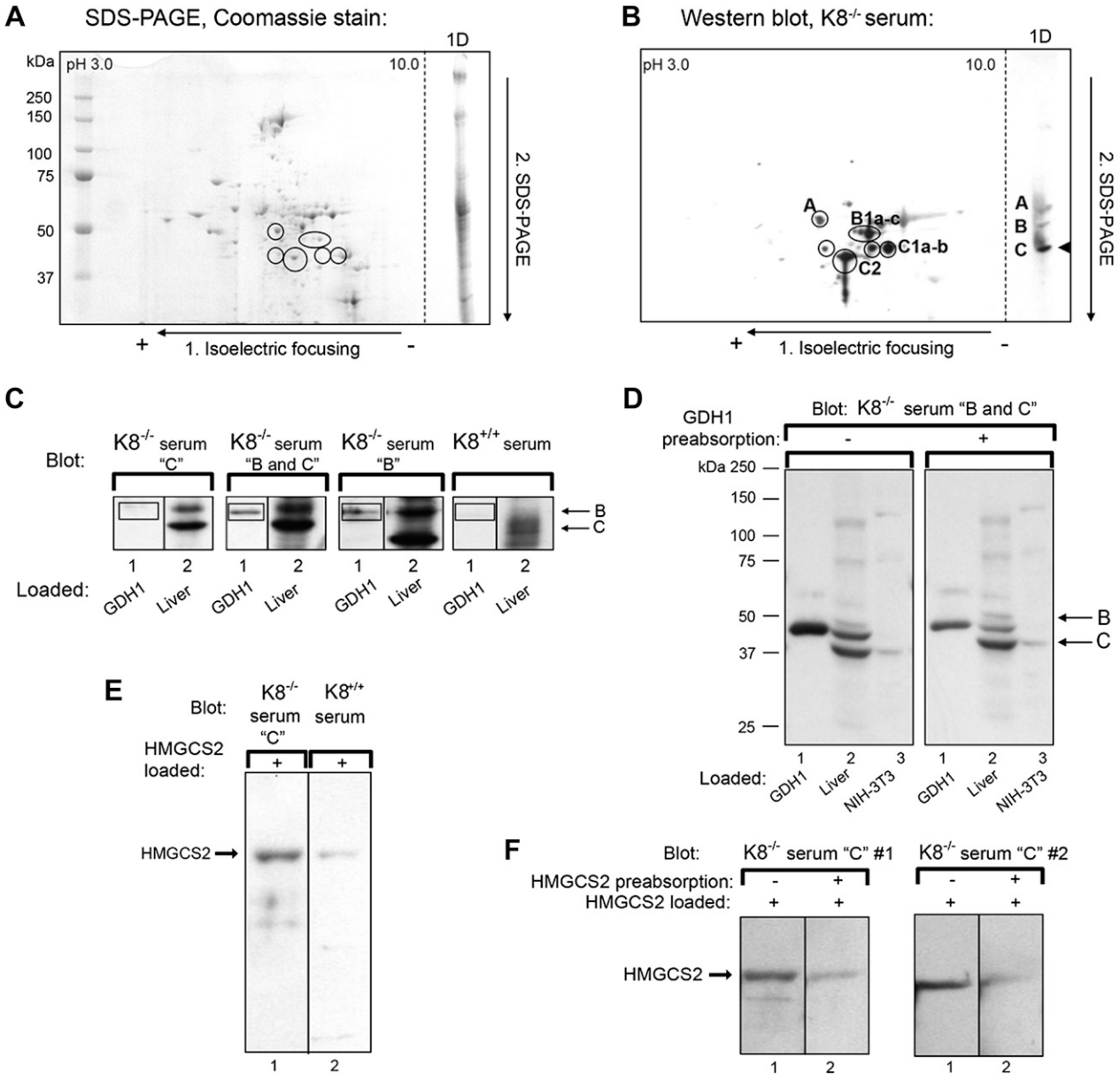

Figure 4. Identification and verification of the K8$^{-/-}$ autoantigens. *A*, *B*) Total mouse liver lysates were separated by isoelectric focusing then SDS-PAGE. Proteins were stained by Coomassie Brilliant Blue (*A*) or blotted with K8$^{-/-}$ serum that recognizes all 4 autoantigens. Liver lysates separated only by SDS-PAGE are included (1D, right side of the panels). *C*) GDH1 (lanes 1) and total liver lysates (lanes 2) were separated by SDS-PAGE on the same gels for each serum, transferred, and analyzed by immunoblotting using K8$^{-/-}$ sera containing the C, B, or C and B autoantibodies, or with K8$^{+/+}$ serum as control. GDH1 is recognized by K8$^{-/-}$ sera containing antibody B but not C (indicated by boxes). *D*) Purified GDH1, liver lysates, and NIH-3T3 lysates were separated on parallel gels and transferred for blotting. Prior to blotting, the K8$^{-/-}$ serum was preabsorbed (right panel) or not (left panel) with GDH1, then used for immunoblotting. *E*) Purified HMGCS2 was immunoblotted with K8$^{-/-}$ serum (lane 1) or K8$^{+/+}$ serum (lane 2). *F*) HMGCS2 was immunoblotted with 2 independent K8$^{-/-}$ sera (serum #1 and serum #2) containing antibody C that had been preabsorbed (lanes 2) or not (lanes 1) with purified HMGCS2. Note that preabsorption leads to a marked reduction in autoantibody reactivity.

another contributing factor may be the altered thymic epithelium in K8$^{-/-}$ mice (46), although this has not been examined in K18$^{-/-}$ or K18 R90C mice and the immunologic consequences of such disruption of the thymic epithelium are unknown. In addition, chronic liver injury per se (up to 8 wk, Supplemental Fig. 1) does not appear to be the culprit in the formation of the autoantibodies, although we cannot exclude the possibility that longer-term chronic injury (which we did not test) may potentially result in autoantibody formation independent of keratin absence or mutation. The implication of our findings is that the defect caused by keratin absence from birth, together with the age effect, promotes antibody formation but in the context of male gender.

The K8$^{-/-}$ mouse autoantigens HMGCS2, catalase, and ALDH E2 are involved in energy metabolism and oxidative stress. HMGCS2, a rate-limiting ketogenic pathway enzyme, is important for energy production under ketogenic

TABLE 2. *Mass spectrometry analysis of K8$^{-/-}$ antigens*

Spot	MW (kDa)	No. of peptides	Score	AA coverage (%)	Protein
A	62	5	94	13	Epoxide hydrolase 2
B1a	61	10	61	22	GDH1
B1b		12	185	27	
B1c		9	131	18	
C1a	57	4	61	7	HMGCS2
B1b		1	16	1	
C1a	57	2	61	5	Catalase
B1b		1	31	2	
C2	53	4	53	7	ALDH E2

AA, amino acid. Spot refers to the 2D protein spots identified and shown in Fig. 4*A* and *B*.

conditions such as starvation (47) and was recently found to be down-regulated in the colon of K8$^{-/-}$ mice (48). Whether such circulating autoantibodies would have pathophysiologic consequences in another organ is not known. The K8$^{-/-}$ mice have colitis, which starts within the first 2 wk after birth (19) indicating that the colitis phenotype is not caused by autoantibody formation. Notably, anti-catalase autoantibodies were reported in 60% of a PSC patient cohort (49) and in rat models of acute fibrosing cholangitis (50). The antioxidant catalase was also found as one of the anti-soluble liver antigens in autoimmune hepatitis type-1 (51). ALDH E2 is important in oxidative stress and part of a large family of NAD(P)+-dependent dehydrogenases (52). Anti-ALDH antibodies are found in cases of unexplained infertility (53) and cancer (54), and ALDH 4A1 levels are significantly changed in K8$^{-/-}$ hepatocyte mitochondria (42). GDH1, a mitochondrial matrix protein with roles in glutamate and energy metabolism, was also identified among the autoantigens. GDH mutations leads to the hyperinsulinism/hyperammonemia syndrome (55), and GDH is up-regulated in liver disease (56). The remaining autoantigen we identified, epoxide hydrolase 2, is a cytoplasmic protein that is important in detoxification (57). Taken together, our findings raise the possibility that AMA may also be found in patients who harbor keratin variants that predispose to liver disease progression or in association with other IF-associated diseases. FJ

The authors thank Hélène Baribault and Thomas Magin for providing the K8$^{-/-}$ and K18$^{-/-}$ mice, respectively, and P. J. Utz for fruitful discussions. Che-Hong Chen is acknowledged for assistance with the 2D-PAGE. The authors also thank Matilda Holm, Neeraj Prabhakar, Jolanta Lundgren, and Helena Saarento for technical assistance. This work was supported by U.S. National Institutes of Health Grants DK47918 (to M.B.O.), K08-DK069385 (to A.H.), DK56339 (Stanford University), and DK34933 (University of Michigan); Academy of Finland #140759/126161 and 266582, Sigrid Juselius Foundation, Liv och Hälsa Foundation, EU FP7 IRG, and ÅAU Center of Excellence (D.M.T.); Turku Doctoral Programme for Biomedical Sciences (J.O.M.); Makarna Agneta och Carl-Erik Olin Foundation (J.H.N.); and the U.S. Department of Veterans Affairs (M.B.O.). The authors declare no conflicts of interest.

REFERENCES

1. Schweizer, J., Bowden, P. E., Coulombe, P. A., Langbein, L., Lane, E. B., Magin, T. M., Maltais, L., Omary, M. B., Parry, D. A., Rogers, M. A., and Wright, M. W. (2006) New consensus nomenclature for mammalian keratins. *J. Cell Biol.* **174**, 169–174
2. Szeverenyi, I., Cassidy, A. J., Chung, C. W., Lee, B. T., Common, J. E., Ogg, S. C., Chen, H., Sim, S. Y., Goh, W. L., Ng, K. W., Simpson, J. A., Chee, L. L., Eng, G. H., Li, B., Lunny, D. P., Chuon, D., Venkatesh, A., Khoo, K. H., McLean, W. H., Lim, Y. P., and Lane, E. B. (2008) The Human Intermediate Filament Database: comprehensive information on a gene family involved in many human diseases. *Hum. Mutat.* **29**, 351–360
3. Omary, M. B., Ku, N. O., Strnad, P., and Hanada, S. (2009) Toward unraveling the complexity of simple epithelial keratins in human disease. *J. Clin. Invest.* **119**, 1794–1805
4. Toivola, D. M., Strnad, P., Habtezion, A., and Omary, M. B. (2010) Intermediate filaments take the heat as stress proteins. *Trends Cell Biol.* **20**, 79–91
5. Pan, X., Hobbs, R. P., and Coulombe, P. A. (2013) The expanding significance of keratin intermediate filaments in normal and diseased epithelia. *Curr. Opin. Cell Biol.* **25**, 47–56
6. Omary, M. B., Coulombe, P. A., and McLean, W. H. (2004) Intermediate filament proteins and their associated diseases. *N. Engl. J. Med.* **351**, 2087–2100
7. Omary, M. B. (2009) "IF-pathies": a broad spectrum of intermediate filament-associated diseases. *J. Clin. Invest.* **119**, 1756–1762
8. Zhong, B., Strnad, P., Selmi, C., Invernizzi, P., Tao, G. Z., Caleffi, A., Chen, M., Bianchi, I., Podda, M., Pietrangelo, A., Gershwin, M. E., and Omary, M. B. (2009) Keratin variants are overrepresented in primary biliary cirrhosis and associate with disease severity. *Hepatology* **50**, 546–554
9. Strnad, P., Lienau, T. C., Tao, G. Z., Lazzeroni, L. C., Stickel, F., Schuppan, D., and Omary, M. B. (2006) Keratin variants associate with progression of fibrosis during chronic hepatitis C infection. *Hepatology* **43**, 1354–1363
10. Strnad, P., Zhou, Q., Hanada, S., Lazzeroni, L. C., Zhong, B. H., So, P., Davern, T. J., Lee, W. M.; Acute Liver Failure Study Group, and Omary, M. B. (2010) Keratin variants predispose to acute liver failure and adverse outcome: race and ethnic associations. *Gastroenterology* **139**, 828–835, 835.e1–835.e13
11. Tao, G. Z., Strnad, P., Zhou, Q., Kamal, A., Zhang, L., Madani, N. D., Kugathasan, S., Brant, S. R., Cho, J. H., Omary, M. B., and Duerr, R. H. (2007) Analysis of keratin polypeptides 8 and 19 variants in inflammatory bowel disease. *Clin. Gastroenterol. Hepatol.* **5**, 857–864
12. Strnad, P., Paschke, S., Jang, K. H., and Ku, N. O. (2012) Keratins: markers and modulators of liver disease. *Curr. Opin. Gastroenterol.* **28**, 209–216
13. Baribault, H., Penner, J., Iozzo, R. V., and Wilson-Heiner, M. (1994) Colorectal hyperplasia and inflammation in keratin 8-deficient FVB/N mice. *Genes Dev.* **8**, 2964–2973
14. Magin, T. M., Schröder, R., Leitgeb, S., Wanninger, F., Zatloukal, K., Grund, C., and Melton, D. W. (1998) Lessons from keratin 18 knockout mice: formation of novel keratin filaments, secondary loss of keratin 7 and accumulation of liver-specific keratin 8-positive aggregates. *J. Cell Biol.* **140**, 1441–1451
15. Toivola, D. M., Nieminen, M. I., Hesse, M., He, T., Baribault, H., Magin, T. M., Omary, M. B., and Eriksson, J. E. (2001) Disturbances in hepatic cell-cycle regulation in mice with assembly-deficient keratins 8/18. *Hepatology* **34**, 1174–1183
16. Gilbert, S., Loranger, A., Daigle, N., and Marceau, N. (2001) Simple epithelium keratins 8 and 18 provide resistance to Fas-mediated

apoptosis. The protection occurs through a receptor-targeting modulation. *J. Cell Biol.* **154**, 763–773
17. Leifeld, L., Kothe, S., Söhl, G., Hesse, M., Sauerbruch, T., Magin, T. M., and Spengler, U. (2009) Keratin 18 provides resistance to Fas-mediated liver failure in mice. *Eur. J. Clin. Invest.* **39**, 481–488
18. Ku, N. O., and Omary, M. B. (2000) Keratins turn over by ubiquitination in a phosphorylation-modulated fashion. *J. Cell Biol.* **149**, 547–552
19. Toivola, D. M., Krishnan, S., Binder, H. J., Singh, S. K., and Omary, M. B. (2004) Keratins modulate colonocyte electrolyte transport via protein mistargeting. *J. Cell Biol.* **164**, 911–921
20. Habtezion, A., Toivola, D. M., Butcher, E. C., and Omary, M. B. (2005) Keratin-8-deficient mice develop chronic spontaneous Th2 colitis amenable to antibiotic treatment. *J. Cell Sci.* **118**, 1971–1980
21. Habtezion, A., Toivola, D. M., Asghar, M. N., Kronmal, G. S., Brooks, J. D., Butcher, E. C., and Omary, M. B. (2011) Absence of keratin 8 confers a paradoxical microflora-dependent resistance to apoptosis in the colon. *Proc. Natl. Acad. Sci. USA* **108**, 1445–1450
22. Mombaerts, P., Mizoguchi, E., Grusby, M. J., Glimcher, L. H., Bhan, A. K., and Tonegawa, S. (1993) Spontaneous development of inflammatory bowel disease in T cell receptor mutant mice. *Cell* **75**, 274–282
23. Kühn, R., Löhler, J., Rennick, D., Rajewsky, K., and Müller, W. (1993) Interleukin-10-deficient mice develop chronic enterocolitis. *Cell* **75**, 263–274
24. Herszényi, L., and Tulassay, Z. (2012) The role of autoantibodies in inflammatory bowel disease. *Dig. Dis.* **30**, 201–207
25. Gossard, A. A., and Lindor, K. D. (2012) Autoimmune hepatitis: a review. *J. Gastroenterol.* **47**, 498–503
26. Hirschfield, G. M., and Gershwin, M. E. (2013) The immunobiology and pathophysiology of primary biliary cirrhosis. *Annu. Rev. Pathol.* **8**, 303–330
27. Ku, N. O., Soetikno, R. M., and Omary, M. B. (2003) Keratin mutation in transgenic mice predisposes to Fas but not TNF-induced apoptosis and massive liver injury. *Hepatology* **37**, 1006–1014
28. Kohli, R., Kirby, M., Xanthakos, S. A., Softic, S., Feldstein, A. E., Saxena, V., Tang, P. H., Miles, L., Miles, M. V., Balistreri, W. F., Woods, S. C., and Seeley, R. J. (2010) High-fructose, medium chain trans fat diet induces liver fibrosis and elevates plasma coenzyme Q9 in a novel murine model of obesity and nonalcoholic steatohepatitis. *Hepatology* **52**, 934–944
29. Hanada, S., Strnad, P., Brunt, E. M., and Omary, M. B. (2008) The genetic background modulates susceptibility to mouse liver Mallory-Denk body formation and liver injury. *Hepatology* **48**, 943–952
30. Strnad, P., Tao, G. Z., Zhou, Q., Harada, M., Toivola, D. M., Brunt, E. M., and Omary, M. B. (2008) Keratin mutation predisposes to mouse liver fibrosis and unmasks differential effects of the carbon tetrachloride and thioacetamide models. *Gastroenterology* **134**, 1169–1179
31. Ku, N. O., Toivola, D. M., Zhou, Q., Tao, G. Z., Zhong, B., and Omary, M. B. (2004) Studying simple epithelial keratins in cells and tissues. *Methods Cell Biol.* **78**, 489–517
32. Nonn, L., Williams, R. R., Erickson, R. P., and Powis, G. (2003) The absence of mitochondrial thioredoxin 2 causes massive apoptosis, exencephaly, and early embryonic lethality in homozygous mice. *Mol. Cell. Biol.* **23**, 916–922
33. Hohenester, S., Beuers, U., Medina, J. F., and Elferink, R. P. (2013) Antimitochondrial antibodies may be insufficiently specific to define primary biliary cirrhosis-like disease in mouse models. *Hepatology* **58**, 828–830
34. Fuchs, E., and Cleveland, D. W. (1998) A structural scaffolding of intermediate filaments in health and disease. *Science* **279**, 514–519
35. Chiorini, J. A., Cihakova, D., Ouellette, C. E., and Caturegli, P. (2009) Sjögren syndrome: advances in the pathogenesis from animal models. *J. Autoimmun.* **33**, 190–196
36. Toivola, D. M., Omary, M. B., Ku, N. O., Peltola, O., Baribault, H., and Eriksson, J. E. (1998) Protein phosphatase inhibition in normal and keratin 8/18 assembly-incompetent mouse strains supports a functional role of keratin intermediate filaments in preserving hepatocyte integrity. *Hepatology* **28**, 116–128
37. Caulin, C., Ware, C. F., Magin, T. M., and Oshima, R. G. (2000) Keratin-dependent, epithelial resistance to tumor necrosis factor-induced apoptosis. *J. Cell Biol.* **149**, 17–22
38. Fickert, P., Fuchsbichler, A., Wagner, M., Silbert, D., Zatloukal, K., Denk, H., and Trauner, M. (2009) The role of the hepatocyte cytokeratin network in bile formation and resistance to bile acid challenge and cholestasis in mice. *Hepatology* **50**, 893–899
39. Loranger, A., Duclos, S., Grenier, A., Price, J., Wilson-Heiner, M., Baribault, H., and Marceau, N. (1997) Simple epithelium keratins are required for maintenance of hepatocyte integrity. *Am. J. Pathol.* **151**, 1673–1683
40. Hanada, S., Snider, N. T., Brunt, E. M., Hollenberg, P. F., and Omary, M. B. (2010) Gender dimorphic formation of mouse Mallory-Denk bodies and the role of xenobiotic metabolism and oxidative stress. *Gastroenterology* **138**, 1607–1617
41. Ku, N. O., Zhou, X., Toivola, D. M., and Omary, M. B. (1999) The cytoskeleton of digestive epithelia in health and disease. *Am. J. Physiol.* **277**, G1108–G1137
42. Tao, G. Z., Looi, K. S., Toivola, D. M., Strnad, P., Zhou, Q., Liao, J., Wei, Y., Habtezion, A., and Omary, M. B. (2009) Keratins modulate the shape and function of hepatocyte mitochondria: a mechanism for protection from apoptosis. *J. Cell Sci.* **122**, 3851–3855
43. Mathew, J., Loranger, A., Gilbert, S., Faure, R., and Marceau, N. (2013) Keratin 8/18 regulation of glucose metabolism in normal versus cancerous hepatic cells through differential modulation of hexokinase status and insulin signaling. *Exp. Cell Res.* **319**, 474–486
44. Tiniakou, E., Costenbader, K. H., and Kriegel, M. A. (2013) Sex-specific environmental influences on the development of autoimmune diseases. *Clin. Immunol.* **149**, 182–191
45. Fallatah, H. I., and Akbar, H. O. (2011) Autoimmune liver disease—are there spectra that we do not know? *Comp. Hepatol.* **10**, 9
46. Odaka, C., Loranger, A., Takizawa, K., Ouellet, M., Tremblay, M. J., Murata, S., Inoko, A., Inagaki, M., and Marceau, N. (2013) Keratin 8 is required for the maintenance of architectural structure in thymus epithelium. *PLoS One* **8**, e75101
47. Hegardt, F. G. (1999) Mitochondrial 3-hydroxy-3-methylglutaryl-CoA synthase: a control enzyme in ketogenesis. *Biochem. J.* **338**, 569–582
48. Helenius, T. O., Misiorek, J. O., Nyström, J. H., Fortelius, L. E., Habtezion, A., Liao, J., Asghar, M. N., Zhang, H., Azhar, S., Omary, M. B., and Toivola, D. M. (2015) Keratin 8 absence down-regulates colonocyte HMGCS2 and modulates colonic ketogenesis and energy metabolism. *Mol. Biol. Cell* **26**, 2298–2310
49. Orth, T., Kellner, R., Diekmann, O., Faust, J., Meyer zum Büschenfelde, K. H., and Mayet, W. J. (1998) Identification and characterization of autoantibodies against catalase and alpha-enolase in patients with primary sclerosing cholangitis. *Clin. Exp. Immunol.* **112**, 507–515
50. Orth, T., Neurath, M., Schirmacher, P., Galle, P. R., and Mayet, W. J. (2000) A novel rat model of chronic fibrosing cholangitis induced by local administration of a hapten reagent into the dilated bile duct is associated with increased TNF-alpha production and autoantibodies. *J. Hepatol.* **33**, 862–872
51. Ballot, E., Bruneel, A., Labas, V., and Johanet, C. (2003) Identification of rat targets of anti-soluble liver antigen autoantibodies by serologic proteome analysis. *Clin. Chem.* **49**, 634–643
52. Yoshida, A., Rzhetsky, A., Hsu, L. C., and Chang, C. (1998) Human aldehyde dehydrogenase gene family. *Eur. J. Biochem.* **251**, 549–557
53. Edassery, S. L., Shatavi, S. V., Kunkel, J. P., Hauer, C., Brucker, C., Penumatsa, K., Yu, Y., Dias, J. A., and Luborsky, J. L. (2010) Autoantigens in ovarian autoimmunity associated with unexplained infertility and premature ovarian failure. *Fertil. Steril.* **94**, 2636–2641
54. Nakanishi, T., Takeuchi, T., Ueda, K., Murao, H., and Shimizu, A. (2006) Detection of eight antibodies in cancer patients' sera against proteins derived from the adenocarcinoma A549 cell line using proteomics-based analysis. *J. Chromatogr. B Analyt. Technol. Biomed. Life Sci.* **838**, 15–20
55. Karaca, M., Frigerio, F., and Maechler, P. (2011) From pancreatic islets to central nervous system, the importance of glutamate dehydrogenase for the control of energy homeostasis. *Neurochem. Int.* **59**, 510–517
56. Ozer, J., Ratner, M., Shaw, M., Bailey, W., and Schomaker, S. (2008) The current state of serum biomarkers of hepatotoxicity. *Toxicology* **245**, 194–205
57. Decker, M., Arand, M., and Cronin, A. (2009) Mammalian epoxide hydrolases in xenobiotic metabolism and signalling. *Arch. Toxicol.* **83**, 297–318

Received for publication December 22, 2014.
Accepted for publication September 8, 2015.